

Electron transport in laterally confined phosphorus δ layers in silicon

S. J. Robinson,^{1,2} J. S. Kline,^{1,2,*} H. J. Wheelwright,¹ J. R. Tucker,² C. L. Yang,³ R. R. Du,³ B. E. Volland,⁴ I. W. Rangelow,⁴ and T.-C. Shen¹

¹Department of Physics, Utah State University, Logan, Utah 84322

²Department of Electrical and Computer Engineering, University of Illinois at Urbana-Champaign, Urbana, Illinois 61801

³Department of Physics and Astronomy, Rice University, Houston, Texas 77005

⁴Department of Electronic and Information Technology, Technical University of Ilmenau, Ilmenau, Germany 98684

(Received 27 July 2006; revised manuscript received 29 September 2006; published 24 October 2006)

Two-dimensional electron systems fabricated from a single layer of P-donors have been lithographically confined to nanometer scale in lateral directions. The electronic transport of such quasi-one-dimensional systems with and without a perpendicular magnetic field was characterized at cryogenic temperatures. Experimental data fit well with two-dimensional weak localization and interaction theory when the phase coherence length is shorter than the smaller dimension of the confinement. Below a transition temperature the wire conductance saturates.

DOI: [10.1103/PhysRevB.74.153311](https://doi.org/10.1103/PhysRevB.74.153311)

PACS number(s): 73.63.-b, 73.20.Fz, 73.43.Qt, 81.16.-c

Since Mott and Twose¹ proposed that electrons moving in a one-dimensional (1D) static potential would be in localized states if there were any disorder in the potential, enormous endeavors and substantial progress have been made to understand the electron transport in reduced dimensions.^{2,3} In particular, advanced lithographic techniques have made it possible to fabricate nanometer-scale metallic 1D systems. The phase coherence lengths obtained from magnetoresistance (MR) measurements of <100-nm wide Al,⁴ Ag,^{4,5} Cu,⁵ Au,^{5,6} Au-Pd,⁷ and Bi (Ref. 8) wires have confirmed the prediction of Al'tshuler *et al.*⁹ that quasi-elastic electron-electron interaction (Nyquist scattering) is the dominant phase-breaking mechanism in 1D at low temperatures. Besides directly depositing thin metal wires on nonconducting substrates, quasi-1D systems can also be realized by constricting a two-dimensional electron gas (2DEG) formed in semiconductors. The Nyquist mechanism has also been observed in narrow Si inversion layers in metal-oxide-semiconductor field effect transistors (MOSFETs)^{10,11} and etched GaAs/AlGaAs heterostructures.¹²

Degenerately δ -doped Si is another 2DEG system. Patterned δ layers have been proposed for sources/drains in field-effect transistors and tunneling devices.¹³ More importantly, they may offer the possibility of 3D integration. In this work, we report studies of electron transport from 2D to quasi-1D δ layers (henceforth, P-donor wires) embedded in crystalline Si. Unpatterned P δ layers, fabricated by adsorbing PH₃ molecules on pristine Si(100)-2 \times 1 surfaces followed by low-temperature Si epitaxial growth, have demonstrated characteristic MR of 2DEGs up to electron densities of 2×10^{14} cm⁻².¹⁴ More recently, P-donor wires have been fabricated by two different contact schemes and successfully characterized by *I*-*V* and MR measurements.^{15,16} We find the wire resistance increases logarithmically at higher temperatures, but saturates below a transition temperature that is correlated to the width of the wire.

Characterization of the P δ -layer was conducted on samples with 8-contact-Hall-bridge mesa configurations etched out from *p*-type Si(100) substrates. The effective width (*W*) and length (*L*) of the Hall bridge is ~ 1 and 5 μ m,

respectively. Below 20 K the substrate acceptors are frozen out and the P δ -layer is electrically isolated from the bulk. At 0.3 K, the typical sheet resistance is ~ 1.4 k Ω /sq. Since $R_{xy}/R_{xx} < 3 \times 10^{-3}$ in the entire magnetic field range, we consider $G = 1/R_{xx}$ throughout this work. Hall measurements determined the electron density to be $\sim 1.3 \times 10^{14}$ cm⁻² with a mobility ~ 34 cm²/V s. The mobility is relatively constant in the temperature range between 0.3 and 20 K. A layer of P-atoms in Si can create strong electrostatic confinement of the donor electrons. A theoretical study¹⁷ shows that at a P-density of 0.2 monolayer, $\sim 35\%$ of these electrons reside in a twofold degenerate Γ -valley with in-plane effective mass $m^* = 0.21m_0$ and the remaining in a fourfold degenerate Δ -valley with in-plane effective mass $m^* = 0.45m_0$, giving a total effective mass $\sim 0.37m_0$. The Fermi level is ~ 0.1 eV below the bulk conduction band minimum and ~ 0.26 eV from the bottom of the Γ -valley. These values, together with the Fermi wave number $\sim 1.6 \times 10^7$ cm⁻¹ and average elastic scattering time (τ) ~ 6.3 fs, determine the diffusion coefficient (*D*) ~ 7.9 cm²/s, and mean free path (*l*) ~ 3.2 nm.

The correction to classical conductivity due to enhanced scattering in a disordered system is a combination of (non-interacting) quantum interference effects and electron-electron Coulomb interaction effects. We will first consider the interference (weak localization) effect which is dictated by the phase-breaking time τ_ϕ . Conventionally, the phase coherence can be broken by inelastic electron-electron interaction, spin-orbit interaction, and magnetic impurity scattering.¹⁸ Assuming the magnetic scattering and spin-orbit interactions are negligible in Si (which will be justified later), τ_ϕ is governed by the inelastic scattering time τ_i . The conductance changes of a 2D sample in a perpendicular magnetic field at a fixed temperature can be written in terms of digamma functions ψ :¹⁹

$$\Delta G_{loc}^{2D}(B) \equiv G(B) - G(0) = \alpha g_v \frac{W}{L} \frac{e^2}{\pi h} \times \left[\psi \left(\frac{1}{2} + \frac{\tau_B}{2\tau_\phi} \right) - \psi \left(\frac{1}{2} + \frac{\tau_B}{2\tau} \right) + \ln \left(\frac{\tau_\phi}{\tau} \right) \right], \quad (1)$$

where $\tau_B = \hbar/2eDB$ is the magnetic scattering time, g_v is the

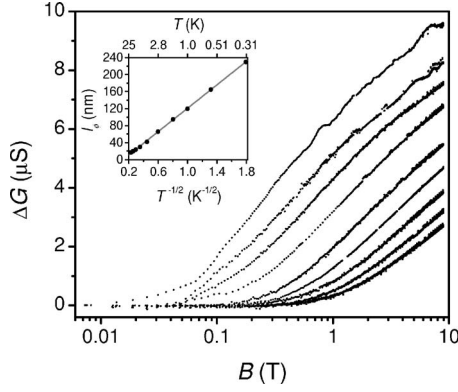


FIG. 1. Change in conductance of a P δ -layer in a perpendicular magnetic field. From top to bottom, $T=0.596, 1.00, 1.55, 2.80, 5.00, 8.04, 11.5, 15.1,$ and 19.0 K. Inset: phase coherent length vs $T^{-1/2}$.

valley degeneracy, and α varies between 1 and $1/g_v$, depending upon the extent of intervalley scattering.²⁰ Figure 1 shows the conductance change of a δ -layer sample at various temperatures in a perpendicular magnetic field. The conductance increases with magnetic field due to the breaking of the time-reversal symmetry that induces localization. At a sufficiently strong field and low temperatures, i.e., $\tau \ll \tau_B \ll \tau_\phi$, the first digamma function in Eq. (1) is close to a constant and the second one is reduced to $\ln B$. When the temperature increases, τ_ϕ decreases and the transition to $\ln B$ dependence shifts to higher fields as can be noted in Fig. 1. For a constant temperature, the interaction effect is not a sensitive function of a weak field; hence, we can determine αg_v and τ_ϕ experimentally by fitting the $B \leq 1$ T portion of the data to Eq. (1) at each temperature. We found that $\alpha g_v = 1.95 \pm 0.07$ at 19 K and 1.27 ± 0.08 at 0.3 K. These results are consistent with the expectation of stronger intervalley scattering at low temperatures.^{20,21} By fitting data to Eq. (1), we can also extract the phase coherence length, $l_\phi = \sqrt{D\tau_\phi}$. We find $l_\phi \propto T^{-1/2}$, as expected from both 2D weak localization and interaction theories.² For $T < 20$ K, both l_ϕ and the electron-electron interaction scale l_T ($l_T \equiv \sqrt{\hbar D/k_B T}$) are much longer than the estimated vertical electron distribution of the P-donor layer (< 2 nm),¹⁷ so the 2D nature of the δ -layer is established.

In addition to localization, we need to consider the effect of electron-electron interactions. To the lowest order, the 2D conductance corrections due to interaction and weak localization are additive. In zero field, the quantum correction to conductance can be written as²

$$\Delta G(T) = G(T) - G(T_0) = \frac{e^2}{\pi h} \left(\frac{W}{L} \right) [\alpha g_v p + \eta_{2D}] \ln \left(\frac{T}{T_0} \right), \quad (2)$$

where p originates from the temperature dependence of τ_i ($\tau_i \propto T^{-p}$) and is determined to be 1 from the earlier discussion, while η_{2D} represents all of the interaction contributions. The $\ln T$ behavior of the conductance change of the δ layers is clearly revealed in Fig. 2. Since the magnetic length $\sqrt{\hbar/eB} \ll l_\phi$ in a 7 T field in the temperature range between

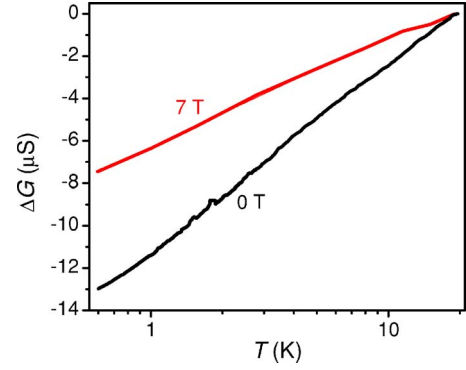


FIG. 2. (Color online) Temperature dependence of the conductance of the P δ -layer.

0.3 and 20 K, the weak localization effect can be ignored and the slope of the 7 T line yields $\eta_{2D} = 0.90 \pm 0.01$ from Eq. (2), which is in line with the result of Sb δ -layer.²¹ At high field and low temperatures, including the Zeeman splitting, η_{2D} can be expressed as $2 - (1 + 2/F) \ln(1 + F/2)$, where $0 \leq F \leq 1$ is the screening factor.² Given $\eta_{2D} = 0.90$, we find $F = 0.43$, suggesting that the screening in the δ -layer is not as efficient as in 3D metallic systems. Applying the values of η_{2D} and p to the zero field data in Fig. 2, we can determine $\alpha g_v = 0.63$, roughly consistent with the results of MR.

The P-donor wires were made from two-terminal device templates consisting of 200 pairs of pre-implanted As contact lines.¹⁵ Low-temperature surface preparation in ultrahigh vacuum²² and scanning tunneling microscope e -beam patterning of H-resist²³ are used to define the wires between a pair of contact lines. PH_3 adsorbs only in the H-desorbed region and hence creates the P-donor wires after Si overlayer growth and activation anneal. The As-implanted contact lines are shown to form ohmic contact with δ layers.¹⁵ The wire resistance is thus determined by a two-terminal method. The three P-donor wires that we report here are fabricated with $W=50, 95,$ and 200 nm and a common $L=750$ nm. The parasitic resistance of As-lines spreads from 100 to 220 k Ω with a median of 132 k Ω , measured by test samples, and only increases by 0.8% from 20 to 0.3 K as depicted in Fig. 3(a). This result indicates that the degenerately doped As-lines are indeed like 3D metals. After subtracting the parasitic resistance [determined self-consistently from Eq. (2)] from the total resistance, the temperature dependence of the conductance change (relative to the conductance at 20 K) of the three P-donor wires is presented in Fig. 3(a). The P-donor wires clearly exhibit two temperature dependencies. At higher temperatures, say $T > 6$ K, all three wires behave like 2D δ layers. Indeed, if we use the same values of η_{2D} and $\alpha g_v p$ obtained from the δ -layer for both zero and 7 T data and the slope of $\Delta G(T)$ for the 95 nm wire, Eq. (2) yields $W/L=0.12$, almost identical with the designed value. The slopes of the 50- and 200-nm wire lead to $W/L=0.087$ and 0.23 , corresponding to a possible 65- and 170-nm physical width, respectively. From the inset of Fig. 1 we find $l_\phi < 39$ nm for $T > 6$ K; hence $l_\phi < W$ and the wires are effectively two-dimensional at sufficiently high temperatures.

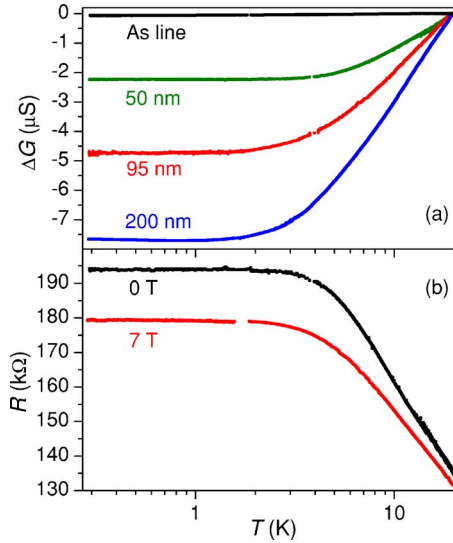


FIG. 3. (Color online) (a) Temperature dependence of the conductance change from 20 K of the 50-, 95-, and 200-nm P-donor wire, and the As^+ implanted electrodes at zero field. (b) The temperature dependence of the resistance of the 50-nm wire at 0 and 7 T magnetic field.

When the temperature decreases below 2.75, 1.23, or 0.59 K, the conductance saturates for the 50-, 90-, and 200-nm wire, respectively. The 2D coherence lengths at these temperatures are 66, 107, and 164 nm comparable to the corresponding wire's physical width. Comparing $R(T)$ of the 50 nm wire in 0 and 7 T fields in Fig. 3(b), we can conclude that the conductance saturation is a combination of localization and interaction effects and the difference of the saturated resistances can be attributed to localization effects.

If the conductance correction of the wires follows the 1D equation²

$$\Delta G = \frac{-e^2}{h} \frac{1}{L} [2\alpha g_v l_\phi + \eta_{1D} l_T], \quad (3)$$

where the first term is from localization and the second term from interaction, we expect a $T^{-1/3}$ dependence of l_ϕ (Ref. 9) and $T^{-1/2}$ dependence of l_T . Conductance saturation thus implies saturation of both l_ϕ and l_T . Figure 4 shows the total MR (including the parasitic MR) of the 50-nm wire unchanged below 2.5 K, indicating that τ_ϕ indeed saturates. In addition, the negative MR implies negligible spin-orbit interaction in our samples.

The saturation of τ_ϕ has been observed in many experiments at ultra-low temperatures²⁴ and extensively reviewed.³ A prominent culprit, magnetic impurities, however, is unlikely to be in our samples, because, as demonstrated in Ref. 5, even with magnetic impurities the wire resistance still varies as $T^{-1/2}$ from the interaction term in Eq. (3). We believe that electron heating is not the reason because the $R(T)$ curve does not change when the driving voltage was reduced from 10 mV to 10 μV and the I - V characteristics are linear up to at least 10 mV. The decoupling of electron-electron thermal equilibrium from the thermal bath due to a lack of electron-phonon scattering²⁵ cannot explain the fact that the same

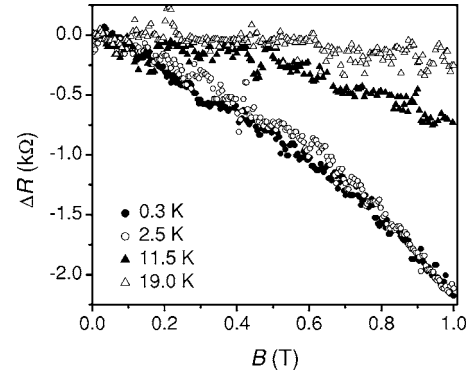


FIG. 4. Temperature dependence of the magnetoresistance of the 50 nm P-donor wire including parasitic resistance of the As-implanted contact.

$R(T)$ can be obtained by either cooling down, heating up or staying at 0.3 K for hours. We also have verified that it is unlikely to have parallel leakage pathways in our systems, because (1) both ^3He and ^4He cryostat generate nearly identical $R(T)$ for $T > 1.6$ K, and (2) the templates have been screened to have over 100 $\text{G}\Omega$ resistance between contacts before nanofabrication in vacuum. If PH_3 exposure creates unintended 1D or 2D conduction pathways, we should observe their characteristic temperature dependence. Since both the l_ϕ 's and l_T 's are within 30% of the designed widths of the P-donor wires when the resistance becomes saturated, we speculate that it is the diffusive boundary of the wires that sets the coherence and interaction length scale. Note that the confinement of the δ layer electrons is estimated to be much weaker in the lateral directions than in the vertical direction.¹³ The extended lateral boundary with low electron density could dominate inelastic scattering that limits the quantum correction to the conductance. Applying the parameters obtained from δ layers and the boundary limited l_ϕ 's to Eq. (3), we find the saturated resistance change between 0 and 7 T of both the 95- and 200-nm wire is within a factor of 3 of the experimental data and a factor of 10 for the 50 nm wire. Resistance saturation in quasi-1D systems near 1 K has also been observed in Bi wires,⁸ and multi-walled carbon nanotubes,^{26,27} but a comprehensive theoretical understanding is still in order.

In conclusion, we have shown that a single layer of P atoms embedded in a Si crystal along the $\langle 100 \rangle$ direction indeed forms a 2DEG system. As in many other 2DEG systems, the electron phase coherence length varies as $T^{-1/2}$ and the resistance has a $\ln T$ dependence. After confining the δ layers into quasi-1D wires, both the phase coherence length and the electron-electron interaction cutoff seem to be limited to the wire width and the wire conductance saturates. More work is required to understand the transport physics of the very narrow δ layers and to improve the conductance for broader device applications.

We would like to thank G. Qian, P. A. Lee, and D. M. Riffe for helpful discussions. This work is supported by the National Science Foundation NIRT Grant No. CCF-0404208.

*Present address: National Institute of Standards and Technology, Boulder, Colorado 80305.

- ¹N. F. Mott and W. D. Twose, *Adv. Phys.* **10**, 107 (1961).
- ²P. A. Lee, *Rev. Mod. Phys.* **57**, 287 (1985).
- ³J. J. Lin and J. P. Bird, *J. Phys.: Condens. Matter* **14**, R501 (2002).
- ⁴S. Wind, M. J. Rooks, V. Chandrasekhar, and D. E. Prober, *Phys. Rev. Lett.* **57**, 633 (1986).
- ⁵F. Pierre, A. B. Gougam, A. Anthore, H. Pothier, D. Esteve, and N. O. Birge, *Phys. Rev. B* **68**, 085413 (2003).
- ⁶P. M. Echternach, M. E. Gershenson, H. M. Bozler, A. L. Bogdanov, and B. Nilsson, *Phys. Rev. B* **48**, 11516 (1993).
- ⁷J. J. Lin and N. Giordano, *Phys. Rev. B* **33**, 1519 (1986); **35**, 545 (1987).
- ⁸D. E. Beutler and N. Giordano, *Phys. Rev. B* **38**, 8 (1988).
- ⁹B. L. Al'tshuler, A. G. Aronov, and D. E. Khmel'nitzkii, *J. Phys. C* **15**, 7367 (1982).
- ¹⁰R. G. Wheeler, K. K. Choi, A. Goel, R. Wisnieff, and D. E. Prober, *Phys. Rev. Lett.* **49**, 1674 (1982).
- ¹¹D. M. Pooke, N. Paquin, M. Pepper, and A. Gundlach, *J. Phys.: Condens. Matter* **1**, 3289 (1989).
- ¹²K. K. Choi, D. C. Tsui, and K. Alavi, *Phys. Rev. B* **36**, 7751 (1987).
- ¹³J. R. Tucker and T. C. Shen, *Solid-State Electron.* **42**, 1061 (1998).
- ¹⁴T.-C. Shen, J.-Y. Ji, M. A. Zudov, R.-R. Du, J. S. Kline, and J. R. Tucker, *Appl. Phys. Lett.* **80**, 1580 (2002); L. Oberbeck, N. J. Curson, M. Y. Simmons, R. Brenner, A. R. Hamilton, S. R. Schofield, and R. G. Clark, *Appl. Phys. Lett.* **81**, 3197 (2002).
- ¹⁵T.-C. Shen, J. S. Kline, T. Schenkel, S. J. Robinson, J.-Y. Ji, C. Yang, R.-R. Du, and J. R. Tucker, *J. Vac. Sci. Technol. B* **22**, 3182 (2004).
- ¹⁶F. J. Ruess, L. Oberbeck, M. Y. Simmons, K. E. J. Goh, A. R. Hamilton, T. Hallam, S. R. Schofield, N. J. Curson, and R. G. Clark, *Nano Lett.* **4**, 1969 (2004).
- ¹⁷G. Qian, Y.-C. Chang, and J. R. Tucker, *Phys. Rev. B* **71**, 045309 (2005).
- ¹⁸S. Hikami, A. I. Larkin, and Y. Nagaoka, *Prog. Theor. Phys.* **63**, 707 (1980).
- ¹⁹C. W. Beenakker and H. van Houten, *Solid State Phys.* **44**, 1 (1991).
- ²⁰H. Fukuyama, *Surf. Sci.* **113**, 489 (1982).
- ²¹S. Agan, O. A. Mironov, E. H. C. Parker, T. E. Whall, C. P. Parry, V. Yu. Kashirin, Yu. F. Komnik, Vit. B. Krasovitsky, and C. J. Emeleus, *Phys. Rev. B* **63**, 075402 (2001).
- ²²J. C. Kim, J.-Y. Ji, J. S. Kline, J. R. Tucker, and T.-C. Shen, *Appl. Surf. Sci.* **220**, 293 (2003).
- ²³T.-C. Shen and Ph. Avouris, *Surf. Sci.* **390**, 35 (1997).
- ²⁴P. Mohanty, E. M. Q. Jariwala, and R. A. Webb, *Phys. Rev. Lett.* **78**, 3366 (1997).
- ²⁵D. J. Bishop, R. C. Dynes, and D. C. Tsui, *Phys. Rev. B* **26**, 773 (1982).
- ²⁶C. Schönenberger, A. Bachtold, C. Strunk, J.-P. Salvetat, and L. Forro, *Appl. Phys. A: Mater. Sci. Process.* **69**, 283 (1999).
- ²⁷J.-O. Lee, J.-R. Kim, J.-J. Kim, J. Kim, N. Kim, J. W. Park, K.-H. Yoo, and K.-H. Park, *Phys. Rev. B* **61**, R16362 (2000).